ELSEVIER

Journal of Power Sources 68 (1997) 623–628

JOURNAL OF POWER SOURCES

Characterization of $Li_{1-\delta}Mn_{2-2\delta}O_4$ defect spinel materials by their phase transition, magnetic and electrochemical properties

Mitsuharu Tabuchi [a,*], Christian Masquelier [b], Hironori Kobayashi [a], Ryoji Kanno [c], Yo Kobayashi [d], Tomoko Akai [a], Yuzuru Maki [e], Hiroyuki Kageyama [a], Osamu Nakamura [a]

[a] *Osaka National Research Institute, 1-8-31 Midorigaoka, Ikeda, Osaka 563, Japan*
[b] *University of Texas at Austin, ETC 9.126, Austin, TX 78712-1063, USA*
[c] *Kobe University, Rokkoudai-cho, Nada, Kobe, Hyogo 657, Japan*
[d] *Central Research Institute of Electric Power Industry, 2-11-1 Iwado-Kita, Komae, Tokyo 201, Japan*
[e] *Rigaku Corporation, 14-8 Akaoji-cho, Takatsuki, Osaka 569, Japan*

Accepted 14 October 1996

Abstract

The effects of both the initial Li:Mn ratio and the Mn valency on the electrochemical and the magnetic properties and on the structural changes were investigated using stoichiometric and nonstoichiometric $LiMn_2O_4$ samples prepared by a solid-state reaction between 673 and 1173 K. A small but known additional plateau near 3.0–3.2 V was observed on discharging the $Li/LiMn_2O_4$ cell using samples with an Mn valency $<3.60+$. However, no plateau at ~ 3.2 V was observed for the cell using samples with an Mn valency of $3.61+$. Below 280 K the structure of the former samples changed from a cubic spinel structure into two phases with a cubic and a tetragonal structure, whereas the structure of the latter, i.e. an Mn^{4+}-rich sample, remained cubic down to 20 K. Therefore, the additional plateau could be correlated with the instability of the cubic spinel structure of the sample. © 1997 Elsevier Science S.A.

Keywords: Lithium manganese oxide spinel; Manganese valency; Jahn–Teller distortion; Magnetic properties

1. Introduction

$LiMn_2O_4$ with a normal spinel structure ($Fd\bar{3}m$) has recently received much attention as the cathode materials for Li rechargeable batteries, because of their low cost and non-toxicity of magnanese, compared with both cobalt and nickel in $LiCoO_2$ and $LiNiO_2$ with the α-$NaFeO_2$-type structure ($R\bar{3}m$) [1–11]. The charge/discharge behavior of the cells using $LiMn_2O_4$ as the cathode material depends strongly on the preparation conditions such as starting material, firing temperature, initial Li:Mn ratio and cooling rate [5,7,9–11]. For a good understanding of the electrochemical properties as a function of the preparation conditions, it is particularly important to characterize the oxidation state of Mn, which, depending on the preparation conditions, can easily vary between an average value of $3.5+$ and $4+$ [9–12]. $Li_2Mn_4O_9$, corresponding to nonstoichiometric $LiMn_2O_4$, was prepared by firing the mixture of Li and Mn carbonates at about 673 K. Kock et al. [13] have found the crystal structure of $Li_2Mn_4O_9$ to be expressed as $Li_{0.89}Mn_{1.78}O_4$ ($\delta = 0.11$, in $Li_{1-\delta}Mn_{2-2\delta}O_4$, δ: amount of cation defects) analyzed by powder neutron diffraction pattern. The concentration of the cation defects decreases irreversibly with increasing firing temperature. Therefore, $Li_2Mn_4O_9$ has been considered as an intermediate phase such as γ-Fe_2O_3 [12]. The large amount of cation defects could be also incorporated into the spinel by means of the initial Li:Mn ratio which is more than 0.5. Gummow et al. [3] reported that the excess Li can substitute the Mn ion on the 16*d* site in the spinel structure. Xia et al. [9] found excellent cycling behavior for nonstoichiometric $Li_{1.0}Mn_{1.93}O_4$ (Li:Mn > 1:2), compared with stoichiometric $LiMn_2O_4$. We examined the effect of the Mn valency on the phase transition and the magnetic properties of various Li–Mn–O samples [14], however, the electrochemical behavior of these samples has still not been examined. By measuring the electrochemical properties, we expect to establish a relation between the physical properties or the phase transition behavior and the electrochemical properties. This work will support the development of Li rechargeable batteries using $LiMn_2O_4$-based cathode material. In this work, we prepared both stoichiometric and nonstoichiometric spinels ($Li_{x(1-\delta)}Mn_{2-2\delta}O_4$, $x = 1.00$, 1.04, and δ: amount of

* Corresponding author.

PII S0378-7753(96)02592-X

cation defects) by solid-state reactions of mixtures of Mn compounds ($MnCO_3$, MnO_2, MnOOH) and Li salts ($LiOH \cdot H_2O$, Li_2CO_3) fired between 673 and 1173 K. We report on the effect of the amounts of defects, and, hence, of the Mn valency, on the structural, magnetic, and electrochemical behavior of selected samples.

2. Experimental

We prepared stoichiometric and nonstoichiometric $LiMn_2O_4$ spinels ($Li_{x(1-\delta)}Mn_{2-2\delta}O_4$, $x=1.00$, 1.04) by a solid-state reaction at 673–1173 K in air, from starting mixtures of either $MnCO_3$, MnOOH or MnO_2 and either Li_2CO_3 or $LiOH \cdot H_2O$, as shown in Table 1. The resulting compositions were determined by chemical analysis based on chemical titration reported by Wickham and Whipple [15] and atomic absorption spectra in order to obtain the exact Mn valence state and Li content, respectively. X-ray diffraction (XRD) measurement were performed by a Rotaflex/RINT (Rigaku), with Si powder used as the internal standard materials. Differential scanning calorimetry (DSC) was measured by a TAS-200 (Rigaku) between 170 and 380 K at a heating and cooling rate of 10 K/min. The magnetic susceptibility of each sample was measured by a Faraday balance (MB-3, Shimadzu) between 83 and 480 K in the field range of 1.8–12.5 kOe. Manganese Tutton's salt ($(NH_4)_2Mn(SO_4)2 \cdot 6H_2O$, reagent grade) was used as the standard calibration material for the magnetic susceptibility measurements. ^7Li MAS (magic angle spinning) NMR spectra were measured at room temperature by a CMX200 (Chemagnetics, $B_0=4.7$ T, $\nu_0=77.828$ MHz) at a spinning rate of 5 kHz. Spectra were obtained by Fourier-transform of the single pulse signal (pulse width: 2 μs and dead time: 4 μs). LiCl powder was used as the standard calibration material for determining the zero chemical shift.

The electrochemical intercalation/de-intercalation reactions were carried out using coin-type cells. The cathode consisted of a mixture of active materials:acetylene black:Teflon powder in 50:10:(0.1–3) mass ratio (mg), pressed into a tablet of 13 mm diameter under a pressure of 9 MPa. The cells used for the electrochemical tests were constructed in a stainless-steel 2016 coin-type configuration. The counter electrode was a disk of Li metal foil (diameter: 15 mm, and thickness 0.24 mm). The separator employed was a microporous polypropylene sheet. The electrolyte used in these cells was a 1 M solution of $LiClO_4$ in a 50:50 mixture of propylene carbonate:1,2-dimethoxymethane (Mitsubishi Petrochemical, battery grade) by volume. The cells were constructed in an argon-filled glove box. The current density (0.5 mA cm^{-2}) was calculated based on the cathode area. The electrochemical measurements were carried out at room temperature between 2.0 and 4.5 V after standing overnight under a zero current flow. The cell properties were measured galvanostatically starting with charging the cell to the 4 V plateau.

3. Results and discussion

We selected seven spinel materials named as S1–S5 for the stoichiometric initial Li:Mn ratio (1.00:2), N1 and N2 for nonstoichiometric Li:Mn ratio (1.04:2), as shown in Table 1. The Mn valency in the sample is higher than 3.53+, when the firing temperatures are below 973 K or when ratios of Li:Mn > 0.5 were used as the starting mixtures. The crystalline phases at about 290 K is also included in Table 1. The samples are single-phased with a cubic spinel structure, except for S1 and S3 which are prepared from the MnOOH–

Table 1
Preparation condition, chemical composition, crystal structure and magnetic data for $Li_{x(1-\delta)}Mn_{2-2\delta}O_4$

Sample	Starting materials	Firing condition	x	n [a]	Chemical formula	Structure at 296 K	$10^5 \chi$ [c] ($cm^3 g^{-1}$)	θ (K)
S1	$2MnOOH + LiOH \cdot H_2O$	673 K + 1173 K, 24 h	1.00	3.505	$Li_{0.999}Mn_{1.998}O_4$	Mixture of cubic, $a=8.24587(16)$ Å and tetragonal, $a=5.8128(6)$ Å, $c=8.2870(12)$ Å	4.49(3)	−277(5)
S2	$4MnCO_3 + Li_2CO_3$	1073 K, 5 h	1.00	3.517	$Li_{0.996}Mn_{1.992}O_4$	Cubic, $a=8.23920(12)$ Å	4.53(3)	−404(4)
S3	$2MnOOH + LiOH \cdot H_2O$	673 K + 973 K, 24 h	1.00	3.526	$Li_{0.994}Mn_{1.988}O_4$	Mixture of cubic, $a=8.2248(3)$ Å and tetragonal, $a=5.8032(4)$ Å, $c=8.2912(6)$ Å	4.36(4)	−297(4)
S4	$4MnCO_3 + Li_2CO_3$	973 K, 5 h	1.00	3.559	$Li_{0.985}Mn_{1.970}O_4$	Cubic, $a=8.24098(14)$ Å	4.44(3)	−219(1)
S5	$4MnOOH + Li_2CO_3$	673 K + 723 K, 24 h	1.00	3.695	$Li_{0.954}Mn_{1.908}O_4$	Cubic, $a=8.204(3)$ Å	5.22(1)	−78(2)
N1	$4MnCO_3 + Li_2CO_3$ [b]	673 K + 1173 K, 24 h	1.04	3.557	$Li_{1.020}Mn_{1.962}O_4$	Cubic, $a=8.23328(6)$ Å	4.48(3)	−253(5)
N2	$4MnCO_3 + Li_2CO_3$ [b]	673 K + 973 K, 24 h	1.04	3.609	$Li_{1.008}Mn_{1.938}O_4$	Cubic, $a=8.2293(2)$ Å	4.58(2)	−212(3)

[a] n is the average valency of Mn ion determined by chemical titration.
[b] Initial Li:Mn ratio was not equal to 1:2, because $MnCO_3$ was slightly hydrated
[c] Magnetic susceptibilities measured at 300 K.
Space group symmetries of cubic and tetragonal phases are $Fd\bar{3}m$ and $I4_1/amd$, respectively.

$LiOH \cdot H_2O$ mixtures above 973 K, and reveal a co-existence of a tetragonal phase ($I4_1/amd$) with this cubic spinel ($Fd\bar{3}m$). However, above 323 K, the structure of both S1 and S3 changes to the cubic structure only. Yamada and Yanaka [16] have firstly reported the formation of the mixture below 282 K. While the lattice parameters of tetragonal phases ($a = 5.7960$ Å and $c = 8.2824$ Å) are very close to our results for the S1 and S3 samples, the phase transition temperatures for the S1 and S3 samples are slightly higher than in Yamada's sample. The difference may be attributed to the different preparation conditions such as starting materials and firing conditions. In fact, a cubic structure for the S2 sample was obtained, in spite of the similarity in the Mn valency observed for the S1, S2 and S3 samples. Precise structural analysis will be needed for explaining the difference.

Charge/discharge characteristics of the $Li/Li_{x(1-\delta)}Mn_{2(1-\delta)}O_4$ cells during the first cycle are shown in Fig. 1. On charging, the plateau near 3.1 V of S1 is longer than of the other samples. As mentioned earlier, XRD at 296 K reveal the S1 sample to consist of a mixed phase, i.e. a cubic ($Fd\bar{3}m$) and a tetragonal ($I4_1/amd$) phase [14], see Table 1. This explains that the occurrence of the plateau is associated with the co-existence of the tetragonal phase and the cubic phase. On discharging, all the cells show discharge plateaus near 2.8 and 4 V. However, a difference in discharge behavior near 3 V was observed: all samples show a plateau near 3 V except for N2 and S5 which have an Mn valency of $>3.61+$. The presence of this plateau has been reported previously [2,7,10] and, Gao and Dahn [10] pointed out that the fraction of this region tends to enlarge with a decrease in the excess amount of Li in $Li_{1+x}Mn_{2-x}O_4$ and the Mn valency [10]. The initial composition and structure of $LiMn_2O_4$ spinels can affect the charge/discharge characteristics.

The change in charge/discharge curves including subsequent cycles is shown in Fig. 2 for Li/N2 and Li/S5 cells. The capacity of the Li/N2 cell decreased with increasing cycle number on both the charge and the discharge. This decrease in capacity is observed for all other samples except for S5. The capacity loss at both 4 and 2.8 V was quite small for Li/S5 cell on increasing the cycle number, despite its smallest capacity during the first cycle. The S5 sample, prepared by firing a stoichiometric mixture of $MnOOH–Li_2CO_3$ at 723 K, has the highest Mn^{4+} content ($n = 3.7$) of our samples, see Table 1. The difference in cycling behavior between Li/S5 cell and the others was similar with the result of Xia et al. [9] whose nonstioichiometric sample ($Li_{1.04}Mn_{2.00}O_{4.14}$, $n = 3.62$) with the Li anode cell has a quite lower capacity loss than an $Li/Li_{1.0}Mn_{1.99}O_4$ ($n = 3.517$) cell. In conclusion, electrochemical measurement showed that the preparation of Mn^{4+}-rich $LiMn_2O_4$ by selecting non-stoichiometric starting mixture (Li:Mn > 1:2) and low firing temperature is an important strategy for optimizing $LiMn_2O_4$ cathode materials.

Fig. 3 shows the DSC curves recorded for seven samples between 170 and 380 K on cooling. For S1–S4 and N1 samples, both exothermic and endothermic (not shown in this figure) peaks were observed at ~280 K on cooling and at

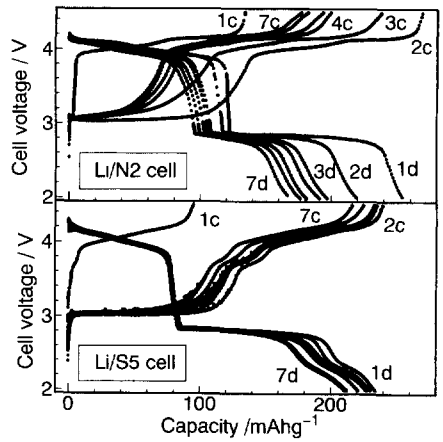

Fig 2 Charge/discharge characteristics of $Li/Li_{x(1-\delta)}Mn_{2-2\delta}O_4$ (N2 and S5 samples) cells for cycle nos. 1–7. For example, 1c and 1d are charge and discharge curves during the first cycle, respectively

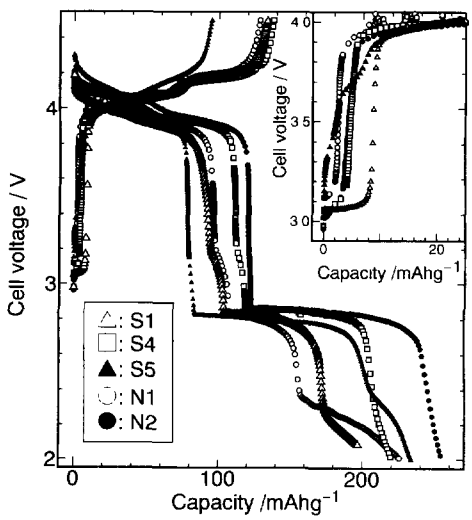

Fig. 1 Charge/discharge characteristics of $Li/Li_{x(1-\delta)}Mn_{2-2\delta}O_4$ cells during the first cycle. Initial charge behavior is emphasized in the inserted figure.

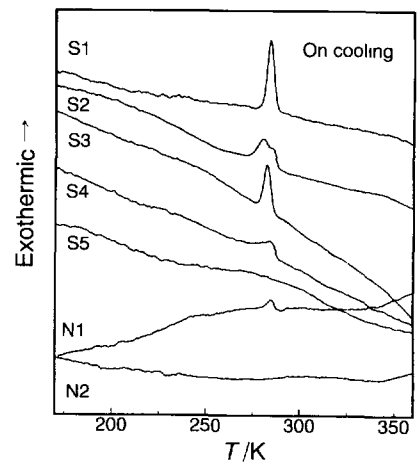

Fig. 3. DSC curves on cooling recorded between 170 and 380 K for $Li_{x(1-\delta)}Mn_{2-2\delta}O_4$ spinels; cooling rate = 10 K/min

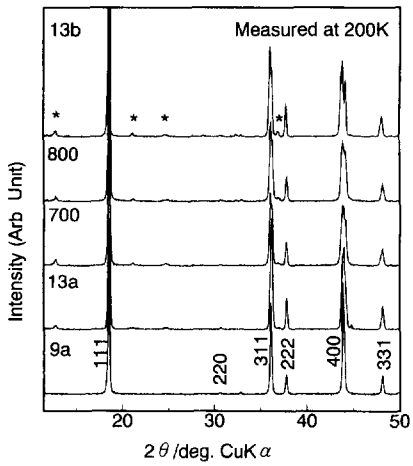

Fig. 4. XRD patterns for $Li_{x(1-\delta)}Mn_{2-2\delta}O_4$ spinels at 200 K. Additional peaks attributed to the tetragonal distortion are marked by asterisks.

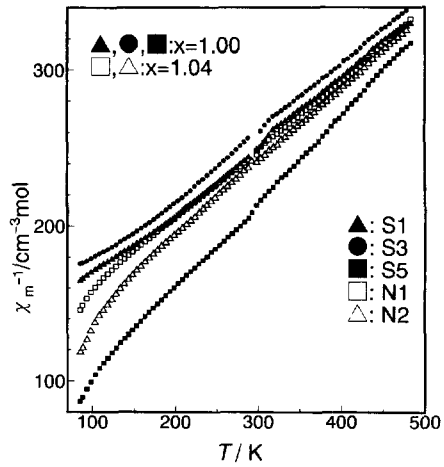

Fig. 5. Temperature dependence of inverse molar susceptibility for $Li_{x(1-\delta)}Mn_{2-2\delta}O_4$ spinels between 83 and 490 K The discontinuous point for each curve is not essential, as it was caused by combining two sets of data, i.e. below and above 300 K.

~303 K on heating, respectively. However, no peaks were observed down to 170 K for S5 and N2 samples with a high Mn valency > 3.60+. The transition observed was attributed to a reversible cubic to cubic+tetragonal transition as reported by Yamada and Tanaka [16]. Splitting of the XRD peaks (especially the (400) peak) except for (111) and (222) peaks was observed for the XRD profile for S1, S2, S4 and N1 samples measured at 200 K (Fig. 4). These splittings were analyzed by a two-phase mixture of the tetragonally distorted ($(c/\sqrt{2}a > 1$) spinel phase ($I4_1/amd$, a = 5.7951(6) Å, c = 8.279(14) Å for S4 sample at 200 K) and the cubic spinel phase ($Fd\bar{3}m$, a = 8.2434(7) Å). However, no peak splitting was observed for the N2 and S5 sample down to 103 K. The DSC exothermic peak, observed for S1, S2, S4 and N1, corresponds to the structural change from the cubic to a two-phase mixture of the cubic and the tetragonal phases. The difference in the phase transition might depend on the amount of Jahn–Teller Mn^{3+} ions ($t_{2g}^3e_g^1$). The additional plateau at ~3.1 V in the discharge curve might also be related to the instability of the cubic structure depending on the cooperative Jahn–Teller effect in the spinel structure. The transition temperature seems to be constant regardless of the different valence states of Mn in DSC curves. The reason is still not clarified. Rogers et al. [17] observed the anomaly of lattice parameters as a function of Mn contents in $Li_{0.5}Fe_{2-x}Mn_xO_4$ and $Li_{0.5}Ga_{2-x}Mn_xO_4$ spinels at $x < 0.3$, and attributed such phenomena to the clustering Jahn–Teller Mn^{3+} ions in order to reduce the elastic energies concerning Jahn–Teller stabilization. This suggests that Mn^{3+} and Mn^{4+} ions in $LiMn_2O_4$ could not distribute randomly on the octahedral 16*d* site, thus the cubic and tetragonal domains are appear <300 K. The difference in Mn valency between nearly stoichiometric samples (S1, S2, S3, S4 and N1) may reflect only the ratio of a tetragonal phase with a fixed composition to a cubic one.

Small XRD peaks marked with asterisks were observed for S1, S2, S4 and N1 samples. Therefore, we tried to index these peaks, in a super-structure of the tetragonal unit cell. These peaks could be indexed by a cell with $a = 3a_0$, $c = c_0$ (a_0 and c_0 are original tetragonal cell ($I4_1/amd$)). Further study on the low temperature structures is now in progress.

Fig. 5 shows the temperature dependence of the inverse molar susceptibility (χ_m^{-1}) for $Li_{x(1-\delta)}Mn_{2(1-\delta)}O_4$. No spontaneous magnetization for each sample was observed even at 83 K, based on the field dependence of magnetization, indicating the absence of ferromagnetic impurities in all samples. Each χ_m^{-1} versus T plot above 200 K could be fitted to a straight line derived from the Curie–Weiss law ($\chi_m^{-1} = (T-\theta)/C_m$, where θ and C_m are the Weiss temperature and Curie constant, respectively). Although no anomaly by phase transition around 290 K could be detected by our measurements, we used each χ_m^{-1} versus T plot above 320 K to calculate two magnetic parameters such as the effective magnetic moment (μ_{eff}) which is calculated from the Curie constant ($\mu_{eff} = (3kC_m/N)^{1/2}$, where k and N represent the Boltzmann constant and Avogadro number, respectively), and the Weiss temperature (θ). The values of μ_{eff} and θ obtained for nearly stoichiometric $LiMn_2O_4$ sample (S1) were 4.28(2) μ_B and −277 K, respectively. These values were close to the previous data which were 4.37 μ_B for μ_{eff} and −260 K for θ [18]. The μ_{eff} value is also close to the expected value 4.42 μ_B for mixed valence state consisting of 50% Mn^{3+} in high spin state ($t_{2g}^3e_g^1$, expected μ_{eff} value is 4.90 μ_B) and 50% Mn^{4+} ($t_{2g}^3e_g^0$, expected μ_{eff} value is 3.87 μ_B). We evaluated the validity of these magnetic parameters by plotting them versus the Mn valency obtained by the wet chemical titration method [15] (Fig. 6). Although these plots were rather scattered, the effective magnetic moment decreased with increasing Mn valency, reflecting the progressive substitution of Mn^{4+} for high-spin Mn^{3+}. The increase in Weiss temperature was also observed with increasing Mn^{4+} content, indicating the progressive change in magnetic interaction from antiferromagnetic to ferromangnetic between Mn ions. This tendency allowed us to explain the increase in contribution of Mn^{4+}–O^{2-}–Mn^{4+} ferromag-

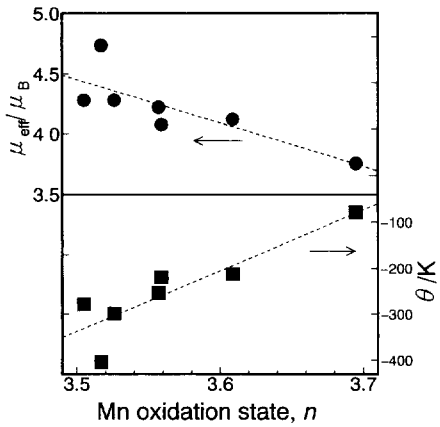

Fig. 6. The Mn valence dependency of the effective magnetic moment (μ_{eff}) and Weiss temperature (θ) for $Li_{x(1-\delta)}Mn_{2-2\delta}O_4$ spinels. The two magnetic parameters for each sample were calculated by fitting χ_m^{-1} vs. T plots above 320 K to a straight line derived from the Curie–Weiss law ($\chi_m^{-1} = (T-\theta)/C_m$).

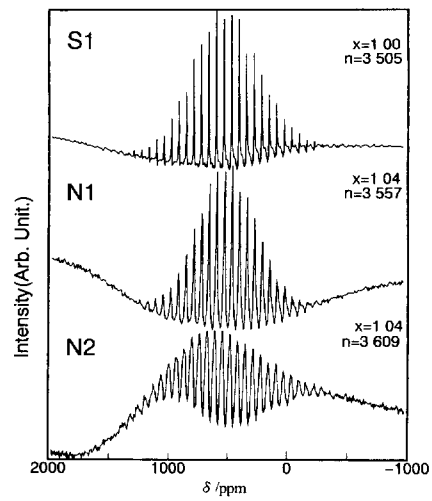

Fig. 7 ^{7}Li MAS NMR spectra of $Li_{x(1-\delta)}Mn_{2-2\delta}O_4$ spinels at room temperature; spinning speed = 5.0 kHz

netic interaction proposed by Blasse [18] to a overall magnetic interaction between Mn ions on the 16*d* sites. The values of μ_{eff} and θ reflect the valence state of Mn ions and magnetic interaction between Mn ions in these spinels, respectively. Thus we can obtain the information about the valence state of Mn in $LiMn_2O_4$ spinels without dissolving the samples for chemical titration.

^{7}Li MAS NMR spectra for three samples named as S1, N1 and N2 were shown in Fig. 7. These spectra for each sample were considered as a single spinning side band manifold centered on 530 ppm and resembled to each other. These spectra are characteristic for paramagnetic solids ($LiNiO_2$ [19], $LiCo_xNi_{1-x}O_2$ [20]) with large isotropic shifts of the resonance, about +500–1000 ppm, which agreed with paramagnetic behavior of these samples. This large positive shift have been attributed as the influence of the interaction between Li and the paramagnetic Ni^{2+} and/or Ni^{3+} ions [20]. These data were quite similar with that of $LiMn_2O_4$ measured by Morgan et al. [21]. They assigned the spectra of $LiMn_2O_4$ as originating from the Li ions at the tetrahedral 8*a* sites. We observed the line broadening with increasing Mn valency. No such sharp NMR band was obtained for S5. Magnetic susceptibility broadening has been considered as a reason of line broadening for paramagnetic solids [22]. Indeed, magnetic susceptibility for S5 at 300 K is quite larger than those of S1, N1 and N2, see Table 1. Thus, the difference in magnetic susceptibility might govern the sharpness MAS–NMR spectra. Marichal et al. [20] pointed out the strong dependence of the line width and the position on the number and magnetic interaction of the 3*d* magnetic ions neighboring Li^+ ion by measuring ^{6}Li and ^{7}Li NMR for samples of $LiNi_{1-y}Co_yO_2$. They obtained a broad NMR spectrum in an Ni-rich sample ($y<0.5$), in spite of the sharp spectra of $LiCoO_2$ which is a diamagnetic compound of low spin Co^{3+} ($t_{2g}^6e_g^0$). In our case, the component of the ferromagnetic interaction, i.e. Mn^{4+} O^{2-} Mn^{4+} increases with increasing Mn^{4+} content (see θ values in Table 1 and Fig. 6). The line broadening with increasing Mn^{4+} content may be affected by the change in magnetic interaction between the Mn ions. More precise and systematic work would be needed for understanding these data.

4. Conclusions

We prepared nearly stoichiometric and nonstoichiometric $LiMn_2O_4$ by a solid-state reaction for investigating different characterization methods of cathode materials, and relating them to the electrochemical properties for rechargeable Li batteries. Understanding the difference in structural change and magnetic property occurring from the cation nonstoichiometry (the amount of cation defects, initial Li:Mn ratio) is a most effective way to screen samples before fabricating the cells using $LiMn_2O_4$ as the cathode material.

Acknowledgements

One of the authors (M. Tabuchi) would like to express his gratitude to Mr Y. Okamura and Dr Y. Takigawa of Osaka Electro-Communication University for fruitful discussion and the preparation of samples. The authors wish to thank Professor H. Yamamura of Kanagawa University for his kindness in offering us γ-MnOOH and for heartfelt advice. The authors are also grateful to Mr A. Kondo of Kobe University for discussions about the electrochemical and the XRD measurements below room temperature. One of the authors (C. Masquelier) gratefully acknowledge financial support by JISTEC (Japan) and the Robert A. Welch foundation (Houston, TX, USA).

References

[1] J.B. Goodenough, M.M. Thackeray, W.I.F. David and P.G. Bruce, *Rev. Chim. Miner.*, *21* (1984) 435–455

[2] J M. Tarascon, W.R. McKinnon, F. Coowar, T.N. Bowmer, G. Amatucci and D. Guyomard, *J. Electrochem. Soc., 141* (1994) 1421–1431.
[3] R.J. Gummow, A. de Kock and M.M. Thackeray, *Solid State Ionics, 69* (1994) 59–67.
[4] V. Manev, A. Momchilov, A. Nassalevska and A Kozawa, *J Power Sources, 43–44* (1993) 551–559.
[5] W.J. Macklin, R.J Neat and R.J. Powell, *J. Power Sources, 34* (1991) 39–49.
[6] M.M. Thackeray, A de Kock, M.H. Rossow and D. Liles, *J. Electrochem. Soc., 139* (1992) 363–366.
[7] A. Yamada, K. Miura, K. Hinomura and M. Tanaka, *J. Electrochem. Soc., 142* (1995) 2149–2156.
[8] H. Huang and P G. Bruce, *J. Power Sources, 54* (1995) 52–57.
[9] Y. Xia, H. Noguchi and M. Yoshio, *J. Solid State Chem., 119* (1995) 216–218.
[10] Y. Gao and J.R. Dahn, *J Electrochem. Soc., 143* (1996) 100–114.
[11] Y. Gao and J.R. Dahn, *Solid State Ionics, 84* (1996) 33–40.
[12] M.M. Thackeray and M.H. Rossow, *J. Solid State Chem., 113* (1994) 441–443.
[13] A. de Kock, M H Rossow, L.A. de Picciotto, M M Thackeray, W I.F David and R.M. Ibberson, *Mater. Res. Bull., 25* (1990) 657–664.
[14] C. Masquelier, M. Tabuchi, K. Ado, R Kanno, Y Kobayashi, Y. Maki, O. Nakamura and J.B. Goodenough, *J. Solid State Chemistry, 123* (1996) 255–266.
[15] D.G. Wickham and E.R. Whipple, *Talanta, 10* (1963) 314–315.
[16] A. Yamada and M. Tanaka, *Mater Res. Bull., 30* (1995) 715–721.
[17] D.B. Rogers, R W. Germann and R J. Arnott, *J. Appl. Phys., 36* (1965) 2338–2342.
[18] G. Blasse, *J. Phys. Chem. Solids, 27* (1966) 383–389.
[19] P. Gangly, V. Ramaswany, I.S. Mulla, R.F. Shinde, P P Bakare, G Ganapathy, P.R. Rajamohanan and N.V.K. Prakash, *Phys. Rev. B, 46* (1992) 11595–11600.
[20] C. Marichal, J Hirschinger, P. Granger, M. Ménétrier, A. Rougier and C. Delmas, *Inorg. Chem., 34* (1995) 1773–1778.
[21] K.R. Mogan, S. Collier, G. Burns and K Ooi, *J. Chem. Soc., Chem. Commun., 1994* (1994) 1719–1720.
[22] M E. Stroll and T.J. Majors, *Phys Rev. B, 24* (1981) 2859–2862.